# Dynamics of topological defects in passive and active liquid crystals

Vincent Hickl

May 12, 2021

## Abstract

Topological defects arise in a variety of physical systems that undergo symmetry-breaking phase transitions into a state of higher order. Liquid crystals (LCs) are a useful set of systems for studying the interactions of multiple defects, particularly their creation and mutual annihilation. In this essay, the basic interactions of defects in LCs are described through the lens of recent experimental and theoretical advances in (quasi-)2-dimensional systems. Then, recent findings in active nematics are described, demonstrating how non-equilibrium interactions can give rise to very different defect behaviors. Unlike equilibrium systems, active nematic liquid crystals can exhibit spontaneous defect creation, leading to turbulent-like dynamics. These systems exemplify how relatively simple interactions between many microscopic objects can lead to complex emergent phenomena at larger scales.

## I. INTRODUCTION

Topological defects can arise in a multitude of physical systems, and are thus of interest to physicists in many subfields, including condensed matter, soft matter, biophysics, and cosmology [1]. Defects commonly arise in symmetry-breaking phase transitions and can play a crucial role in establishing long-range order. Defect structures can be very complex and their dynamics highly non-trivial. Thus, it is very useful to study defects in a generic theoretical framework, yielding a universal description that can then be applied to a variety of different physical systems. Defects are fundamentally an emergent phenomenon, as they describe the organization of many small constituents of a a physical system. Since these constituents can have many different properties, it is highly desirable for the universal description to be independent of the short-scale properties of any specific system being studied. By formulating a purely macroscopic theory of defect dynamics, universal behavior can be identified effectively.

Nevertheless, experimental verification is crucial to test the predictions of such a theory, as it necessarily requires certain approximations to be made when neglecting the microscopic details of a system. To this end, model systems that allow for easy observation and quantification of defects are used. Liquid crystals are a prime candidate, as the defects they form can easily be observed with optical microscopy. There are many types of liquid crystal, including mixtures of organic molecules, polymers, or even living cells. Most consist of molecules or cells that are approximately rod-shaped and can thus be described by a director field.

Liquid crystals can form different phases as they are cooled down from an isotropic state and become more ordered. The one with the highest energy is the nematic phase, where rod-shaped molecules have orientational order (they align along a common axis), but no positional order in three dimensions [2]. If the system is cooled further, smectic phases may arise, where molecules organize into distinct layers in three dimensions. In each layer, molecules are aligned as in the nematic phase. Smectic A refers to the case where molecules are aligned perpendicular to the layer, whereas Smectic C refers to the case where there is some non-zero angle between the alignment and the layer normal. Additional phases include chiral phases, twisted nematics, and discotic and conic phases for molecules that are disk- and cone-shaped, respectively. If a liquid crystal is cooled down quickly enough, different regions within the material may not be in thermal contact with each other. This process, sometimes called thermal quenching, leads to spatial gradients of the molecular orientation, and can cause topological defects to appear.

Active matter describes systems made of many small constituents that exchange energy with each other and their surroundings. Thus, active matter gives rise to phenomena that cannot be described by equilibrium statistical mechanics. Activity often leads to collective motion, in which the constituents of a system display long-range ordering on scales much larger than their physical size. Examples famously range across many scales, from subcellular microtubules to flocks of birds [3]. In the case of liquid crystals, activity fundamentally alters the behavior of a system, as it no longer necessarily tends towards thermodynamic equilibrium. As a result, topological defects can be created spontaneously, and new kinds of long-range ordering can occur.

In this essay, the dynamics of topological defects in both passive and active liquid crystals are described. For the sake of simplicity, the discussion is restricted to 2D and quasi-2D systems, where 3D defect structures like dislocations cannot exist. Additionally, the 3-

dimensional structure that distinguishes nematic, smectic, and other phases need not be considered. In the passive case, "dynamics" primarily refers to the motion of two defects, especially those of opposite topological charge which eventually annihilate. For active liquid crystals, much more complex motion may arise. In both cases, the basic theory commonly used to model the systems is described. Then, experimental techniques and results of interest are discussed. Ultimately, the behavior of defects in liquid crystals is placed into the broader context of universality in physical systems and the concept of emergent physical phenomena.

## II.   DEFECTS IN PASSIVE LIQUID CRYSTALS

Two-dimensional liquid crystals can be described by a 2D director field $\hat{n}(x, y)$ for nematic, smectic, and isotropic liquid crystals alike. The elastic free energy density $w$ of a director field can be written as

$$w = \frac{1}{2} \left[ K_S (\nabla \cdot \hat{n})^2 + K_T (\hat{n} \cdot \nabla \times \hat{n})^2 + K_B (\hat{n} \times \nabla \times \hat{n})^2 \right], \tag{1}$$

where $K_S$, $K_T$, $K_B$, are the elastic constants for splay, twist, and bend, respectively [1]. In 2D there is no twist, so only the first and last terms remain. It is often useful to make one-constant approximation $K_S = K_B = K$, which yields

$$w = \frac{K}{2} \left[ \left( \frac{\partial \theta}{\partial x} \right)^2 + \left( \frac{\partial \theta}{\partial y} \right)^2 \right]. \tag{2}$$

Thus, the lowest energy configuration in a simple, passive liquid crystal is for all the molecules or cells to align, such that any spatial derivatives of $\theta$ vanish.

### A.   Theory of passive defect dynamics

In general, a topological defect is a discontinuity in a field that cannot be removed by a local change in the field. In the case of a 2-dimensional director field, a topological defect refers to a singularity in the field with some non-zero topological charge $S$, defined as the number of full rotations of the director on a closed path around the singularity. Such a defect also has a phase, $\theta_0$, which is the angle between a vector pointing from the defect core to a nearby point and the director at that point (Fig. 1). Thus, the director field near a defect at the origin is given by

$$\theta(\vec{r}) = S\phi(\vec{r}) + \theta_0, \tag{3}$$

where $\phi(\vec{r})$ is the polar coordinate of the point defined by $\vec{r}$, and $\hat{n} = (\cos \theta, \sin \theta)$. Determining the director field near two defects becomes very difficult when they do not share the same phase. To solve this problem, Tang and Selinger showed that an arbitrary defect with charge $S$ can be represented by a tensor of order $n|1 - S|$, where $n$ can be any integer [4]. Using the technique of conformal mapping, they were able to derive analytical solutions for

2
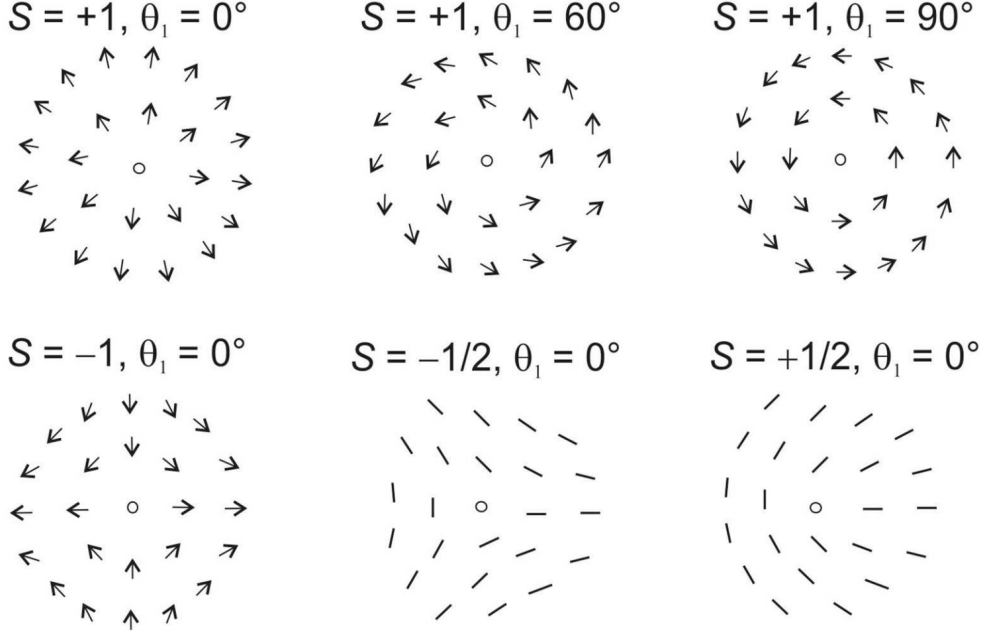
FIG. 1. Sketches of topological defects with strengths $\pm 1$ and $\pm 1/2$ with different phases $\theta_1$. The phase of $+1$ defects changes their structure qualitatively (see top row images). For all defects of strengths $S \neq 1$, a non-zero phase $\theta_1$ is equivalent to a simple rotation of the defect by an angle $\theta_1/(1-S)$. Reproduced from Harth and Stannarius (2020).

the director field around two defects in the one-constant approximation:

$$\theta(\vec{r}) = S_1 \tan^{-1}\left(\frac{y-y_1}{x-x_1}\right) + S_2 \tan^{-1}\left(\frac{y-y_2}{x-x_2}\right) + \frac{\delta\theta}{2}\left[1 + \frac{\log\left(|\vec{r}-\vec{R}_1|^2/|\vec{r}-\vec{R}_2|^2\right)}{\log\left(|\vec{R}_1-\vec{R}_2|^2/r_c^2\right)}\right] + \Theta$$

(4)

where

$$\delta\theta = \theta_2 - \theta_1 + S_2 \tan^{-1}\left(\frac{y_1-y_2}{x_1-x_2}\right) - S_1 \tan^{-1}\left(\frac{y_2-y_1}{x_2-x_1}\right)$$

(5)

$$\Theta = \theta_1 - S_2 \tan^{-1}\left(\frac{y_1-y_2}{x_1-x_2}\right)$$

(6)

Here $S_1$ and $S_2$ are the defects' charges, $\theta_1$ and $\theta_2$ their phases, $R_1$ and $R_2$ their positions, and $r_c$ is the size of the defect core, i.e. the region where orientational order is disrupted. Typically one assumes that the core size is much smaller than the separation between defects. From this expression, the elastic free energy for a system if size $R_{max}$ can be calculated:

$$w = \pi K(S_1+S_2)^2 \log\left(\frac{R_{max}}{r_c}\right) - 2\pi K S_1 S_2 \log\left(\frac{|\vec{R}_1-\vec{R}_2|}{2r_c}\right) + \frac{\pi K \delta\theta^2}{2}\frac{\log\left(|\vec{R}_1-\vec{R}_2|/(2r_c)\right)}{[\log\left(|\vec{R}_1-\vec{R}_2|/(r_c)\right)]^2}.$$

(7)

The first term is the energy cost of a defect pair with net charge $S_1 + S_2$. The second term indicates that defects of like charge repel one another, while those of opposite charge attract.

The third term represents a preferential alignment of the defects such that their phase is the same, meaning $\delta\theta = 0$. As a result, there is an aligning torque which causes defects to follow a curved path as they move apart or towards each other.

These effects, which cause topological defects to move, are balanced by a drag force. For the simplified case using the one-constant approximation and negligible flow, the drag is given by

$$F_{drag} = \pi\gamma_1 S^2 v \log(L/r_c) \tag{8}$$

where $\gamma_1$ is the rotational diffusivity and $L$ is the characteristic system size. The logarithmic divergence of this expression is addressed by imposing a long-distance cut-off, giving

$$F_{drag} = \pi\gamma_1 S^2 v \log(3.6/Er) \tag{9}$$

where $Er = \gamma_1 v r_c/K$ is called the Ericksen number. Ultimately, the velocity of the defects is found to be

$$v = \pm\frac{K}{\gamma_1 \log(3.6/Er)R}. \tag{10}$$

Thus, as defects of oppose charge attract each other, their separation varies as $R(t) \propto t^{1/2}$.

In real systems, one must consider additional corrections, such as those due to material flow, finite system size, or elastic anisotropy ($K_S \neq K_B$). According to a recent review, a general description of defect dynamics that incorporates all of these aspects is still missing [1]. Nevertheless, some of the consequences of these corrections have been known qualitatively for some time. For example, both elastic anisotropy and flow-coupling cause positive defects to move faster than their negative counterparts.

### B.   Experimental results

A system particularly well-suited for observations of defects in a quasi-2D LC is a freely suspended Smectic C [5]. Smectic phases possess positional order in one dimension, meaning the molecules are organized into distinct layers with a well-defined thickness. Each layer forms an independent 2D system in which the projection of each molecule's orientation into the film plane (called the c-director) plays the role of the director field described above. The orientation of the c-director also determines the polarization of light passing through it, so the director field can be determined by observing the film using crossed polarizers, sometimes with the addition of a diagonal $\lambda$ wave plate. Specifically, the apparent color of the film changes based on the local orientation of the c-director.

The trajectories of topological defects as they annihilate were visualized as described above by Missaoui et al. [5] in a Smectic C film made from 50:50 wt% 5-n-octyl-2-[4-(n-hexyloxy)phenyl]-pyrimidine and 5-n-decyl-2-[4-(n-octyloxy) phenyl]-pyrimidine (Fig. 2). When the film first forms, it takes on the lowest energy configuration where all molecules are aligned with no defects. Disclinations are subsequently created by touching the film with a thin fiber ("hair tip"). The initial alignment is random, and it is not possible to distinguish between the directions $\vec{n}$ and $-\vec{n}$. One direction is simply chosen, and is used consistently throughout each experiment so that it does not affect the conclusions. The defects shown are initially both mismatched and misaligned, causing their trajectories to be curved. Because of elastic anisotropy, the +1 defect (red line in Fig.3 (c)), moves fast than the -1 defect (blue line). As predicted by theory, these experiments also show that $\delta\theta$

4
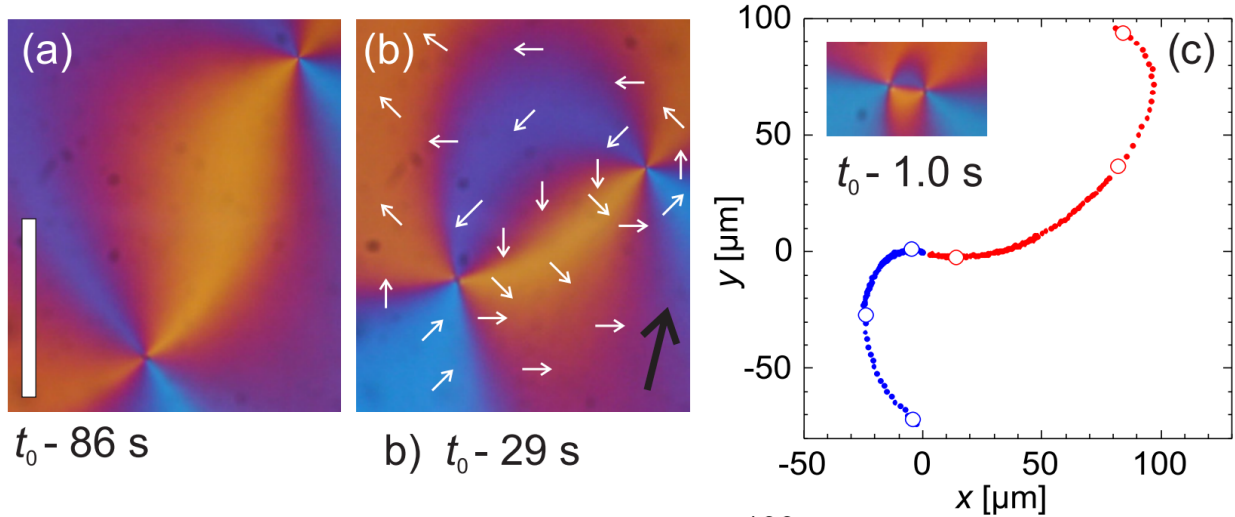
FIG. 2. (a),(b) Mismatched (initial $\delta\theta \approx 65°$) and misaligned (initial $\delta\phi \approx -36°$) defect pair on the way to annihilation. White arrows sketch the c-director. The +1 defect (top) is $\approx 1.8$ times faster than the -1 defect. The black arrow indicates the outer director field. (c) Trajectories respective to the annihilation point. Circles mark the defect positions in frames (a)–(c). Adapted from Missaoui et al. (2020).

and $\delta\phi$, are linear dependent. However, the data suggest that $\delta\theta \approx -\delta\phi$, in disagreement with the theoretical prediction of $\delta\theta \approx -2\delta\phi$. The precise reason for this discrepancy remains unclear. Other authors have suggested that it may be due to deviations from the one-constant approximation, or that the finite film size affects pair orientation [1].

In a system with many defects, pair annihilation leads to coarsening of the overall system. Interestingly, the pattern of defects remains self-similar, meaning that zooming in on a part of the director field at some time is indistinguishable from looking at the whole field at a later time. In 2D, the predicted scaling of the defect density $\rho$ is $\rho(t) \propto t^{-1}$. One of the first experimental verifications of this scaling behavior came from a study that, surprisingly, was motivated mainly by cosmology [6]. In short, the Kibble-Zurek mechanism describes how large-scale structures in the universe can be explained by the existence of a symmetry-breaking phase transition in the very early universe. In this scenario, the supercooling of a two-component scalar field (the Higgs fields) would create cosmic strings — one-dimensional topological defects. While experiments cannot be conducted on cosmological scales, cosmologists soon realized that important insights could be gained by studying other systems with the same *scaling behavior*, such as certain liquid crystals.

In this spirit, experiments were conducted by Chuang et al. using the nematic liquid crystal knows as K15 [6]. The isotropic-to-nematic transition was induced by applying a pressure jump $\Delta P$, which causes $+1/2$ defects, or "strings," to form. The length of strings per unit volume is analogous to the defect density $\rho$, as well as the density of cosmic strings in the Kibble-Zurek mechanism. As expected, the scaling follows $\rho(t) \propto t^{-1}$. It must be noted that while the system is three-dimensional, the string density is measured per unit area in two-dimensional images. Thus, one can write $\rho \equiv 1/\xi^2$, where $\xi$ is a characteristic length scale. At any time, the nematic liquid crystal in these experiment can be characterized by a single length scale, meaning it remains self-similar (Fig. 3). Crucially, this means that if the scaling of $\rho$ with time is known, the structure of the system at any point in the past
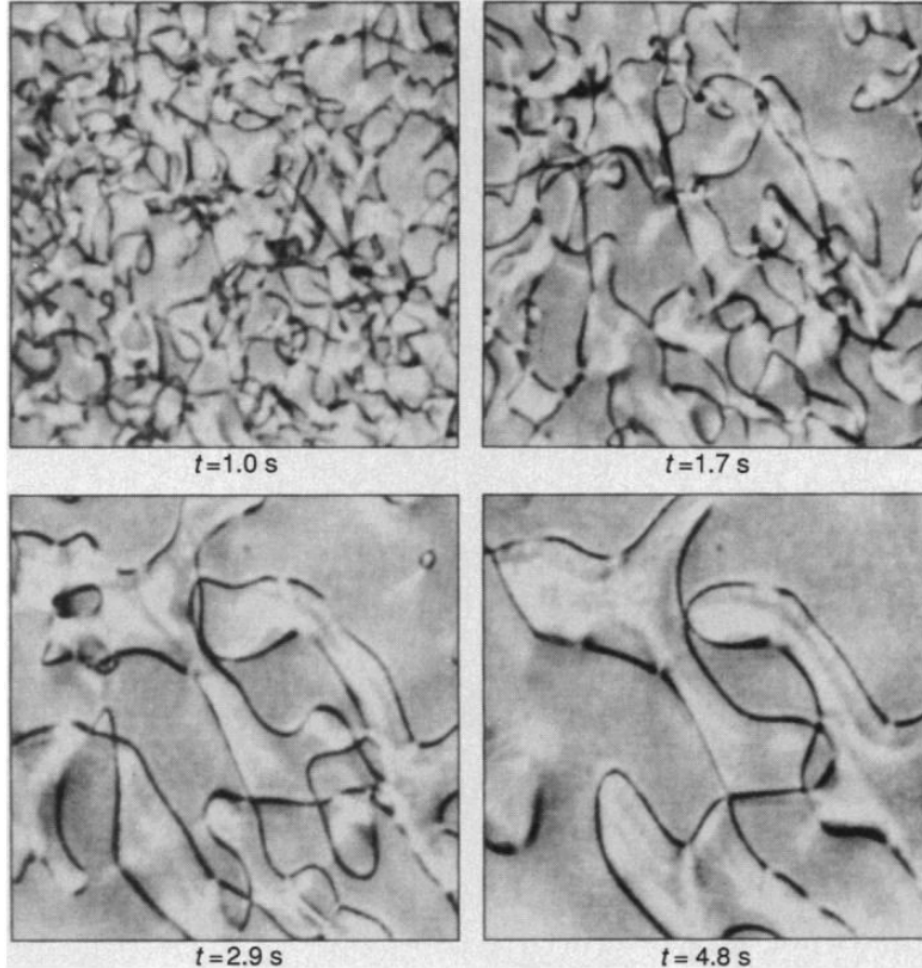
FIG. 3. A coarsening sequence showing the strings visible in a nematic liquid crystal, at t = 1.0, 1.7, 2.9, and 4.8 seconds after a pressure jump of $\Delta P$ from an initially isotropic state in equilibrium at approximately 33°C and 3.6 MPa. The evolution of the string network shows self-similar or "scaling" behavior. Each picture shows a region 360 μm in width. Adapted from Chuang et al. (1991).

(such as the structure of the universe moments after the big bang) can easily be deduced, as long as the present structure can be observed.

This example perfectly illustrates why the study of universal scaling laws is so useful. In the authors' own words, "the universality of symmetry-breaking phenomena suggests that theories [...] beyond the grasp of human manipulation may nevertheless be explored by observing similar systems in which all the relevant length scales have been uniformly scaled."

## III.   DEFECTS IN ACTIVE LIQUID CRYSTALS

In an active liquid crystal, the components that make up the crystal can exchange energy with each other or their surroundings. As a result, and unlike the systems described above, active LCs do not necessarily tend towards a uniform director field in which topological

defects annihilate. Instead, defect pairs can be created spontaneously before moving along chaotic trajectories and eventually annihilating [7, 8]. In this section, the formation of topological defects in active liquid crystals and their dynamics are described. A full theoretical description is beyond the scope of this work. Instead, we briefly present the equations governing the time evolution of a 2D director field before focusing on a qualitative description of the emergent physics and a description of recent experimental advances.

## A. Theory and simulation of defect formation

There is a standard expression for the Landau-de Gennes free energy functional of a director field in the one-constant approximation [8]:

$$\mathcal{F} = \frac{K}{2}(\partial_k Q_{ij})^2 + \frac{A}{2}Q_{ij}Q_{ji} + \frac{B}{3}Q_{ij}Q_{jk}Q_{ki} + \frac{C}{4}(Q_{ij}Q_{ji})^2. \tag{11}$$

Here $\boldsymbol{Q}$ is the order parameter tensor of the director field. This free energy is used to obtain the so-called molecular field $H_{ij}$:

$$H_{ij} = -\frac{\delta\mathcal{F}}{\delta Q_{ij}} + \frac{\delta_{ij}}{3}\operatorname{Tr}\left(\frac{\delta\mathcal{F}}{\delta Q_{kl}}\right). \tag{12}$$

This field in turn is used to write down the standard evolution equation for $\boldsymbol{Q}$, which describes the hydrodynamics of a liquid crystal:

$$(\partial_t + u_k\partial_k)Q_{ij} - S_{ij} = \Gamma H_{ij}. \tag{13}$$

Here $S_{ij}$ is an advection term which can be written in terms of the strain rate tensor $E_{ij} = (\partial_i u_j + \partial_j u_i)/2$, the vorticity tensor $\Omega_{ij} = (\partial_j u_i - \partial_i u_j)/2$, and the order parameter tensor, and $\Gamma$ is a constant. From all this, one obtains the equations of motion for the velocity field of the director $\vec{u}$:

$$\nabla \cdot \vec{u} = 0; \qquad \rho(\partial_t + u_k\partial_k)u_i = \partial_j \Pi_{ij} \tag{14}$$

where $\rho$ is the fluid density and $\boldsymbol{\Pi}$ is the stress tensor. The full expression for $\boldsymbol{\Pi}$ is fairly complicated, and depends on all of the quantities defined so far in this section, as well as the pressure and viscosity of the fluid. For a passive LC, $\boldsymbol{\Pi}$ includes two terms: the viscous stress, which depends only on the viscosity and the strain rate, and the passive stress, which combines all other terms. To incorporate activity, one simply adds an active term

$$\Pi_{ij}^{active} = -\alpha Q_{ij} \tag{15}$$

where $\alpha$ controls the strength of the activity. As a result of this activity, any gradient in $\boldsymbol{Q}$ produces a flow. Extensile flow arises when $\alpha > 0$, and contractile flow arises when $\alpha < 0$. The way topological defects form in an initially uniform director field was shown by Thampi et al. using numerical simulations based on equations (13) and (14) for a system with extensile flow [8]. Small bend fluctuations are reinforced by local shear, forming so-called "walls" in the director field (Fig. 4 (a)-(c)). The dominant length scale of these deformations is given by the strength of the elastic forces relative to the activity: $\sqrt{K/\alpha}$. As the director tilts further, two defects of charge $+1/2$ and $-1/2$ are formed inside each wall where the tilt is strongest. Subsequently, defects move around following complex trajectories dictated by
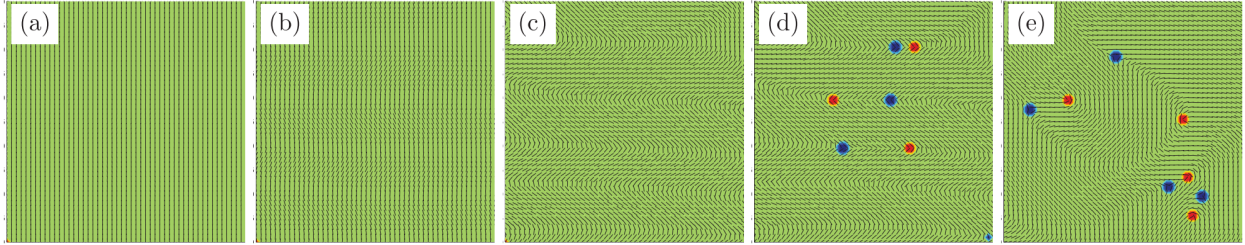
FIG. 4. Snapshots at successive times of the director field (dashed lines) and +1/2 and -1/2 defects (red and blue, respectively) during the development of active turbulence from an ordered nematic state for an extensile system. Two stages are seen: walls are formed ((b), (c)), local nematic order is restored by the formation of pairs of defects ((d), (e)). Reproduced from Thampi et al. (2014).

the physics in section II as well as the activity of the director field.

## B.   Experimental results

Experimentally, active liquid crystals can be observed in a variety of systems. One prominent example is that of kinesin motors bound to microtubules, which play an important part in cellular processes such as cytoskeleton formation and cell division. A quasi-2D active liquid crystal can be created by depositing an aqueous solution of microtubules and kinesin onto an oil film, as was done by Opathalage et al. [9]. In these experiments, surfactants are used to stabilize the oil-water interface, allowing the microtubules form a dense nematic film. Microtubules are able to slide relative to one another, while also being bound into bundles by the kinesin and an added depletion agent, polyethylene glycol. Finally, the aqueous phase contains an ATP-generating system, providing a constant source of energy. Kinesin motors use energy obtained from the consumption of ATP to "walk" along microtubule bundles, causing bundle extension, which is the source of the activity (extensile flow) in the nematic film.

The overall topological charge of the nematic film is determined by the boundary conditions of the system. The oil on which the microtubules are confined to circular holes in a photoresist, giving the film a net charge of +1 (sometimes called the Euler characteristic). As a result, the nematic field must contain at least two +1/2 defects. The strength of the confinement was varied by changing the diameter $D$ of the circle, leading to drastically different behaviors, which the authors categorize as intermediate, strong, and weak confinement. These behaviors are summarized in Fig. 5.

Under intermediate confinement ($D = 200$ µm), two +1/2 defects orbit one another in a spiral pattern centered on the center of the circle. Note that the size of a defect, defined by the minimum radius of curvature of the microtubules, was $r_c \approx 100$ µm. As the two defects approach each other near the center, a pair of one +1/2 and one -1/2 defect is formed at the system boundary. This state is destroyed shortly thereafter, as one of the original two +1/2 defects and the -1/2 defect annihilate each other. The two remaining defects then continue to orbit each other, until the process repeats. The lifetime of the created defect pair is about an order of magnitude less than the time between creation events.

Under strong confinement ($D \leq r_c = 100$ µm), defects could no longer be identified as the microtubules accumulate along the boundary of the system. Nevertheless, circular
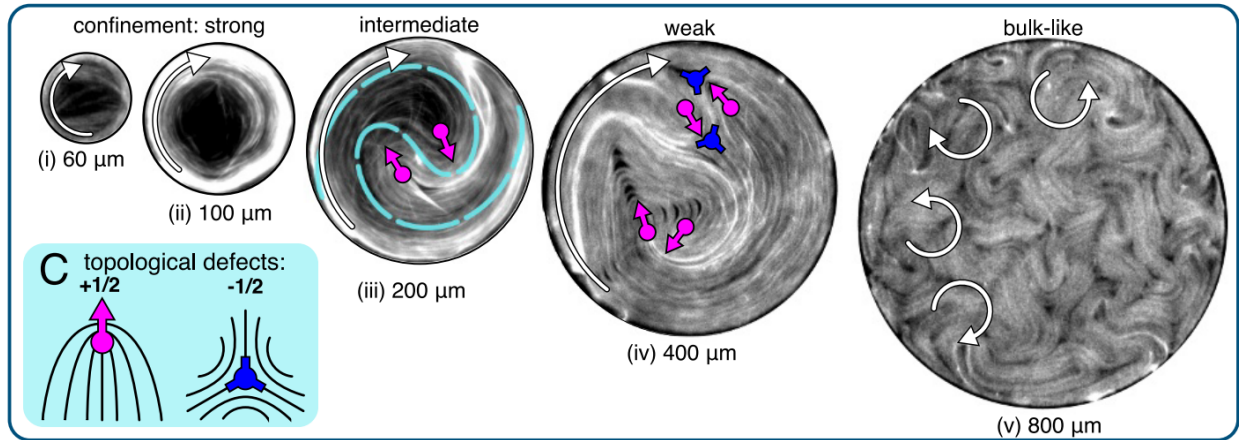
FIG. 5. Fluorescence images of confined active nematics with diameters of (i) 60, (ii) 100, (iii) 200, (iv) 400, and (v) 800 µm. White arrows indicate direction of circulation. Cyan line overlaying the 200 µm disk highlights the double spiral configuration of the nematic director observed for intermediate confinements. Photographs are not to scale. (C) Structure of nematic director field around topological defects of charge +1/2 (magenta) and -1/2 (blue). Adapted from Opathalage et al. (2019).

rotations of the microtubules remained even for $D = 60$ µm, driven by the activity induced by the kinesin motors. This result is interesting because theory predicts that circulation should cease for sufficiently small confinements, where elastic effect impeding the motion dominate. The authors do not state what the cause of this discrepancy would be. Perhaps even stronger confinement would stop the rotation.

Under weak confinement ($D > 400$ µm), defects pairs can form both at the boundary and within the bulk of the nematic. These defects exhibit chaotic dynamics as they orbit and annihilate one another. Nevertheless, a strong overall flow circulation remains for diameters up to $D = 600$ µm. The direction of flow can occasionally flip from clockwise to counter-clockwise, or vice-versa, but the time scale for this change is 1-2 orders of magnitude greater than the typical timescale on which defect creation/annihilation occurs. As predicted by hydrodynamic theory, the density of defects drops off sharply as the system diameter increases from the strongly confined to the weekly confined regime, and then levels off under further increases of $D$. However, this leveling off does not coincide with the disappearance of circular flow, as predicted by theory. In experiments, circular flow persists for significantly larger sizes. The authors argue that this discrepancy is caused by the defect pairs created at the boundary, which align themselves with existing circular flow, and in turn produce active stresses that further stabilize the motion.

The experimental design described above can, in principle, be used to study various different geometries with different boundary conditions. The importance of confinement in determining defect dynamics means that the geometry and size of the system can be used to control active nematics in general. It is worth emphasizing that all the phenomena describes in this section of are ultimately the result of the interactions of kinesin motors and microtubules on the scale of nanometers and microseconds. Yet, without explicitly considering any of the details of these interactions, an accurate description of the dynamics over hundreds of microns and several minutes was obtained.

9
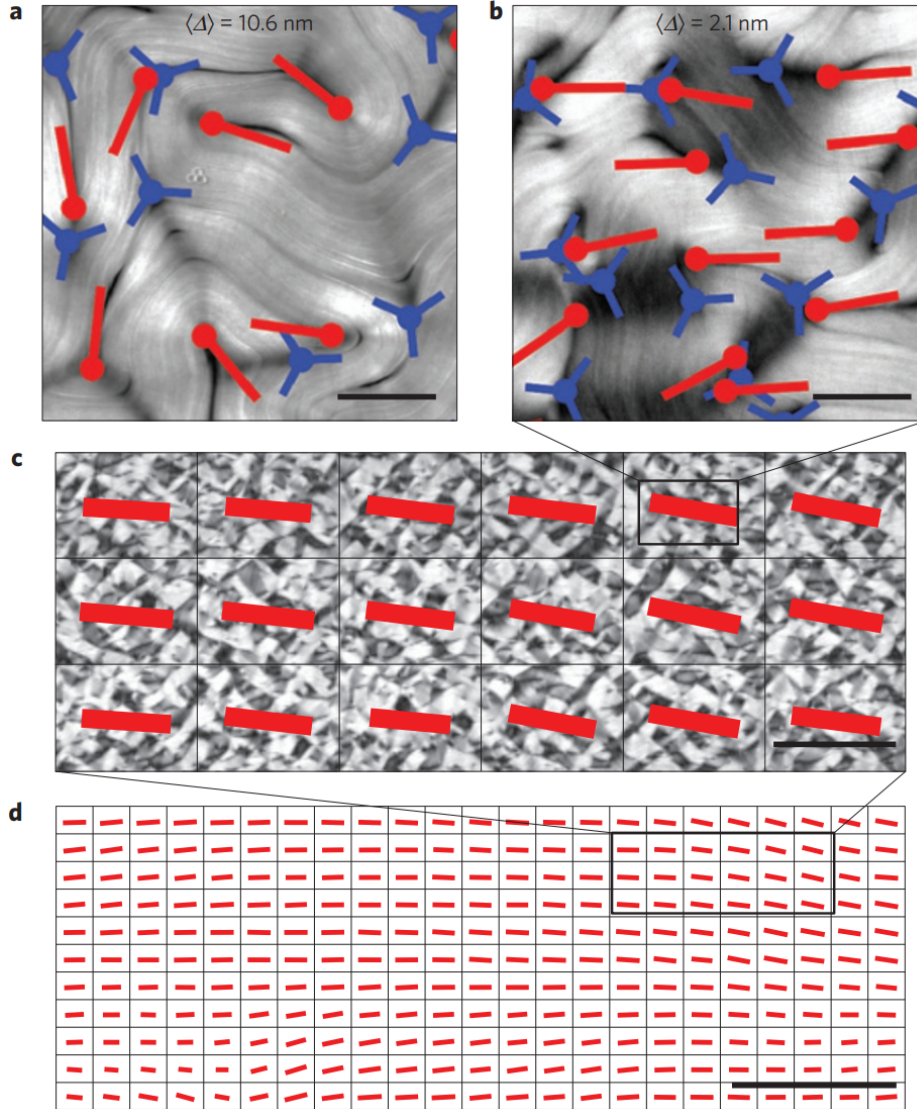
FIG. 6. **a**, Retardance map of a thick microtubule (MT) film in the regime of weak defect alignment. Red and blue markers indicate locations and orientations of $+1/2$ and $-1/2$ defects. Scale bar, 200 μm. **b**, Thin MT film showing strong alignment of $+1/2$ defects. Scale bar, 200 μm. **c**, Orientational order in a large active-nematic sample. Each red bar's orientation and length indicates the mean direction and strength of the defect alignment in one field of view. Scale bar, 2 mm. **d**, Defect alignment spans the largest samples studied (6 cm × 2 cm), containing ~20,000 defects. Scale bar, 10 mm. Adapted from DeCamp et al. (2015).

At the largest system sizes examined in this study ($D = 800$ μm), there is not net circulation, and defects follow trajectories that appear chaotic. Because of the visual resemblance to turbulent fluid flow, this motion is usually called "active turbulence" [3]. Experiments on active turbulence in microtubule films over even larger spatial scales (up to a few centimeters, with thousands of defects) have shown that long-range orientational ordering of the defects can persist for several hours [10]. Since this long-range order was observed in both experiments and simulations of a generic 2D nematic, the authors suggest it may be

a generic feature of active nematics. Remarkably, at these large scales, the coarse-grained defect alignment looks very similar to a uniform director field (Fig. 6 c and d, where each director represents the mean direction of all defects in a certain region of space). It is tempting to suggest that the array of these mean orientations could itself behave like a liquid crystal, demonstrating a kind of scale invariance. However, more experiments would be required before such claims can be made.

In systems with contractile flow ($\alpha < 0$, activity can also lead to defect proliferation [8]. However, in the case of a pair of $\pm 1/2$ defects, contractile flow speeds up the motion of the defects towards each other by driving the $+1/2$ defect in the direction of its "tail" [7]. This process enhances the annihilation of defects already observed in passive liquid crystals. The extensile flow discussed previously has the opposite effect by driving defects in the direction of their "head." Nevertheless, when defects annihilate in a system with contractile flow, the resulting uniform director field is unstable. The activity leads to the creation of additional defect pairs, eventually giving rise to active turbulence.

## IV. SUMMARY AND OUTLOOK

In this work, a broad overview of how topological defects interact in liquid crystals was given. The basic theory was described briefly, before being illustrated with examples from recent experimental and computational studies. In passive liquid crystals, defects of opposite charge attract and annihilate under the influence of elastic stresses balanced by drag on the underlying director field. This process iteratively leads to coarsening of the defect patterns, which remain self-similar as their characteristic length scale changes. In active systems, defects can proliferate, especially when the active flow is extensile. The creation of additional defects leads to active turbulence, which can be controlled by confining the system. At very large scales, orientational order of defect orientations in active nematics has been observed. These phenomena are generally considered to be universal for many different systems containing topological defects. Thus, the relative ease with which experiments can be conducted in liquid crystalline systems makes them a useful tool for many physical areas of research.

It must be said that, in this work, we have only scratched the surface of the existing literature on liquid crystals. Countless experimental, computational, and theoretical studies have been performed describing the various details of defect interactions. Many details of the dynamics have been neglected here for the sake of brevity. Active liquid crystals in particular are the subject of a rapidly growing literature since many biological systems, including colonies of bacterial or epithelial cells, display nematic order. Activity in these systems can arise either from self-propulsion or cell division [11].

Many open questions remain specifically with regards to how different defect dynamics arise when the properties of the underlying constituents are changed. Addressing this problem requires taking into account multiple length scales. Since the study of 2D systems allows for certain simplifications, there is even more progress to be made when studying 3D systems. In the long term, there is widespread hope that an improved understanding of defect interactions and dynamics can be used to control active processes both in biological and synthetic systems [3]. Two important ways this goal could be achieved is with confinement (as discussed above), or by controlling the properties of the microscopic active constituents, either via bioengineering or by constructing artificial micromachines. Needless to say, the study of topological defects in liquid crystals is a thriving research topic, with an

ever-growing list of potential applications.

---

[1] Kirsten Harth and Ralf Stannarius. Topological Point Defects of Liquid Crystals in Quasi-Two-Dimensional Geometries. *Frontiers in Physics*, 8:1–19, 2020.

[2] Denis Andrienko. Introduction to liquid crystals. *Journal of Molecular Liquids*, 267:520–541, 2018.

[3] Amin Doostmohammadi, Jordi Ignés-Mullol, Julia M. Yeomans, and Francesc Sagués. Active nematics. *Nature Communications*, 9:3246, 2018.

[4] Xingzhou Tang and Jonathan V. Selinger. Orientation of topological defects in 2D nematic liquid crystals. *Soft Matter*, 13:5481–5490, 2017.

[5] Amine Missaoui, Kirsten Harth, Peter Salamon, and Ralf Stannarius. Annihilation of Point Defect Pairs in Freely Suspended Liquid-Crystal Films. *Physical Review Research*, 2:1–8, 2019.

[6] Isaac Chuang, Ruth Durrer, Neil Turok, and Bernard Yurke. Cosmology in the laboratory: Defect dynamics in liquid crystals. *Science*, 251:1336–1342, 1991.

[7] Luca Giomi, Mark J. Bowick, Xu Ma, and M. Cristina Marchetti. Defect annihilation and proliferation in active Nematics. *Physical Review Letters*, 110:228101, 2013.

[8] Sumesh P. Thampi, Ramin Golestanian, and Julia M. Yeomans. Instabilities and topological defects in active nematics. *EPL*, 105:1–6, 2014.

[9] Achini Opathalage, Michael M. Norton, Michael P.N. Juniper, Blake Langeslay, S. Ali Aghvami, Seth Fraden, and Zvonimir Dogic. Self-organized dynamics and the transition to turbulence of confined active nematics. *Proceedings of the National Academy of Sciences of the United States of America*, 116:4788–4797, 2019.

[10] Stephen J. DeCamp, Gabriel S. Redner, Aparna Baskaran, Michael F. Hagan, and Zvonimir Dogic. Orientational order of motile defects in active nematics. *Nature Materials*, 14:1110–1115, 2015.

[11] Amin Doostmohammadi, Sumesh P. Thampi, Thuan B. Saw, Chwee T. Lim, Benoit Ladoux, and Julia M. Yeomans. Celebrating Soft Matter's 10th Anniversary: Cell division: a source of active stress in cellular monolayers. *Soft Matter*, 11:7328–7336, 2015.